Non-Hermitian superfluid–Mott-insulator transition in the one-dimensional zigzag bosonic chains

Chengxi Li [1,2] Yubiao Wu [1] and Wu-Ming Liu [1,2,3,*]

[1]*Beijing National Laboratory for Condensed Matter Physics, Institute of Physics, Chinese Academy of Sciences, Beijing 100190, China*
[2]*School of Physical Sciences, University of Chinese Academy of Sciences, Beijing 100049, China*
[3]*Songshan Lake Materials Laboratory, Dongguan, Guangdong 523808, China*

(Received 18 September 2023; revised 29 April 2024; accepted 28 May 2024; published 14 June 2024)

We investigated the behavior of non-Hermitian bosonic gases with Hubbard interactions in one-dimensional (1D) zigzag optical lattices through the calculation of dynamic response functions. Our findings showed the existence of a non-Hermitian quantum phase transition that is dependent on the pseudo-Hermitian symmetry. The system tends to exhibit a superfluid phase when subjected to weak dissipation. While under strong dissipation, the pseudo-Hermitian symmetry of the system is partially broken, leading to a transition toward a normal liquid phase. As the dissipation increases beyond the critical threshold, the pseudo-Hermitian symmetry is completely broken, resulting in a Mott-insulator phase. We propose an experimental setup using 1D zigzag optical lattices containing two-electron atoms to realize this system. In this paper, we emphasize the key role of non-Hermiticity in quantum phase transitions and offer a theoretical framework as well as experimental methods for understanding the behavior of dissipative quantum systems, implicating significant development of quantum devices and technologies.

DOI: 10.1103/PhysRevB.109.214306

I. INTRODUCTION

The superfluid (SF)–Mott-insulator (MI) phase transition in strongly correlated gases has been widely studied [1–4]. In recent years, zigzag bosonic chains have been mainly researched for strongly correlated quantum phase transitions and Majorana fermions [5]. This system contains various MI phases and gapless SF phases, forming a rich phase diagram [6–8]. At the same time, the system also helps us to understand magnetic models and can be experimentally verified by implementing ultracold atoms in optical lattices [9–12]. In zigzag bosonic chains, the paired Bose-Hubbard model can be realized. Unlike the Bose-Hubbard model, the paired Hubbard model introduces a pairing contribution, which creates and annihilates boson pairs on adjacent lattice sites. This pairing contribution may lead to the appearance of the Z_2 phase and topological properties [6,13,14]. Therefore, this model provides rich resources for physical intuition and the connection with magnetic models [15].

In recent years, significant advancements have been made in the study of non-Hermitian systems [16]. Notably, key characteristics of non-Hermitian phase transitions in specific SF systems have been elucidated [17]. Concurrently, other research has delved into the conditions under which periodically driven quantum systems manifest a stable subharmonic response in the presence of dissipation [18]. Furthermore, in the domain of atomic and optical systems, an experimental realization of a non-Hermitian spin-orbit-coupled Fermionic system has been successfully achieved [19].

However, research on one-dimensional (1D) zigzag bosonic chains faces a number of challenges in non-Hermitian systems. Firstly, the eigenvalues and eigenvectors of the system no longer have real properties, making the determination of phase transitions more complex [20–22]. Secondly, the properties of the SF and MI phases of the system may also change. For example, the coherence of the SF phase may be lost, while the localization of the MI phase may become more pronounced [16,23]. Finally, in terms of experiments, there are also challenges in the implementation and control of the 1D zigzag bosonic chains in non-Hermitian systems. For instance, different methods are required for the preparation and control of this model due to the nonreal energy in non-Hermitian systems [24]. Additionally, dissipation in non-Hermitian systems may have an impact on experimental results, necessitating more sophisticated experimental design and control.

In this paper, we propose and investigate non-Hermitian 1D zigzag bosonic chains in ultracold atoms. This paper was inspired by a recent series of non-Hermitian transport discoveries [20–22,25–30]. We utilized the theory of non-Hermitian linear response to calculate the Green's function of our system at zero temperature [31,32]. By applying Kubo's formula, we analyzed the evolution and phase transition of the non-Hermitian system under external perturbation and discovered that the non-Hermitian phase transition is accompanied by symmetry breaking. We found that the SF-MI phase transition can be effectively controlled by dissipation. These findings provide important insights for understanding phase transitions and critical phenomena in non-Hermitian many-body systems.

II. NON-HERMITIAN ZIGZAG BOSONIC CHAINS

Our experimental setup consists of two-level bosons with internal states $|g\rangle$ and $|e\rangle$ situated in a 1D zigzag optical lattice. A typical lattice scheme is illustrated in Fig. 1(a) for

*Contact author: wmliu@iphy.ac.cn

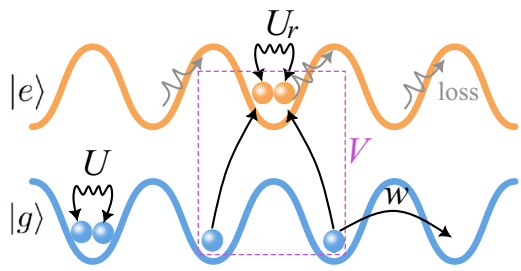

FIG. 1. Implementation of non-Hermitian paired Bose-Hubbard model in the zigzag optical lattices. A stable (dissipative) optical lattice is applied to the ground (excited) state $|g\rangle$ ($|e\rangle$). w is the hopping term for the $|g\rangle$ chain, and the interchain interaction V can induce the pair hopping via an energy-conserving process. The on-site interaction strength is $U\,(U_r)$ for the $|g\rangle$ ($|e\rangle$) chain. A running wave parallel to an optical lattice couples $|g\rangle$ to $|e\rangle$, which undergoes rapid on-site loss, giving rise to the non-Hermitian pair-hopping process.

^{174}Yb, where the two levels are encoded in the atomic states $^1S_0 = |g\rangle$ and $^3P_0 = |e\rangle$. Utilizing specific laser wavelength $\lambda_L = 1120$ nm of the optical lattice, for which the polarizations of $|g\rangle$ and $|e\rangle$ are opposite [33,34], we can generate internal-state-dependent potentials, and the potential minima for the $|g\rangle$ chain locate in the middles of each of those for the $|e\rangle$ chain. The excited state is assumed to be unstable with a loss rate, and the chain loaded with $|e\rangle$ is treated as a reservoir chain for concentrating on the $|g\rangle$ chain of interest, and it can be described by the non-Hermitian paired Bose-Hubbard Hamiltonian:

$$H = -\sum_{\langle i,j\rangle}(w b_i^\dagger b_j + \text{H.c.}) + V b_i^\dagger b_j^\dagger b_{ij,R} b_{ij,R} + \sum_i \left[\frac{U}{2} n_i(n_i-1) - \mu_0 n_i\right]. \quad (1)$$

Here, $b_i(b_i^\dagger)$ is the annihilation (creation) operator for atoms in the $|g\rangle$ chain at site i with density operator $n_i = b_i^\dagger b_i$, and $b_{ij,R}$ and $b_{ij,R}$ are for atoms in the reservoir chain at the site between ground chain site i and j. Here, w is the hopping magnitude, and U is the on-site interaction strength for the $|g\rangle$ chain. Also, μ_0 is the tunable chemical potential offset between two chains, and the chemical potential of reservoir chain is shifted to zero. The pair hopping is introduced by an energy-conserving process mediated by interchain interaction V.

The basic idea behind the atomic implementation of pairing terms can be engineered by applying a laser beam resonant to the energy difference, which offsets the interaction energy U_r of two bosons on the reservoir chain and the chemical potential offset μ_0 between the chains. Thus, single-particle interchain tunneling is suppressed, and resonant pair tunneling to or from a single site on the reservoir chain dominates, contributing a nonnegligible quartic bosonic process and effectively giving a pairing term on the $|g\rangle$ chain. By employing the mean-field approach to treat the interaction terms, we can obtain the order parameters $\Delta_{ij,1} = V\langle b_{ij,R} b_{ij,R}\rangle \approx \Delta_1$ and $\Delta_{ij,2} = V\langle b_{ij,R}^\dagger b_{ij,R}^\dagger\rangle \approx \Delta_2$. Since the effective term depends on the expectation value of the pair annihilation or creation process on the reservoir chain with an on-site loss rate, the pairing parameters will be imbalanced, and we define them as unequal real parameters which can be obtained by $U(1)$ transformation.

In the strongly interacting limit, the Hilbert space of our system can be restricted to the number-basis states $|n_0\rangle$ or $|n_0+1\rangle$ at each sites. Such a hard-core bosonic model can be transformed into a magnetic model using the operator representation $s = \frac{1}{2}$, $|n_0+1\rangle = |\uparrow\rangle$, $|n_0\rangle = |\downarrow\rangle$ by defining $b_i^\dagger b_j \to (n_0+1)s_i^+ s_j^-$, $n \to n_0 + s^z + \frac{1}{2}$. Using degenerate perturbation theory to second order of w/U, the transverse field XY model can be derived, with complex anisotropic spin-exchange integrals J_x and J_y, and Zeeman magnetic field h, see the Appendixes [6]. Then it can be transformed into the quasifermionic effective Kitaev model (EKM) by a Jordan-Wigner transformation $s_i^+ = c_i^\dagger \exp(-i\pi\sum_{j<i} c_j^\dagger c_j)$, see the Appendixes, in the $t/U \to 0$ limit, i.e., $H = \sum_{\langle i,j\rangle} -t c_i^\dagger c_j + \text{H.c.} + \Delta c_i^\dagger c_j^\dagger + \gamma c_i c_j + \sum_i \mu c_i^\dagger c_i$. Here, $t = (n_0+1)w$ is the nearest-neighbor hopping amplitude, $\Delta = (n_0+1)\Delta_1$ and $\gamma = (n_0+1)\Delta_2$ denote the strength of pair parameters between the nearest-neighbor sites, and μ is the on-site renormalized chemical potential. Although the SF order parameters in this case are complex, they can always be transformed into real values through a unitary transformation, see the Appendixes. In the following, we calculate the linear response of the EKM to investigate the physical properties of our system near the MI regime.

III. PSEUDO-HERMITIAN SYMMETRY

Under periodic boundary conditions, the $\mathcal{PT}$ symmetry-breaking Hamiltonian becomes $H(k) = \xi(k)\sigma_z/2 + (\Delta+\gamma)\sigma_x/2 + i(\Delta-\gamma)\sigma_y/2$, with $\xi(k) = \mu - 2t\cos k$, and $\sigma_{x,y,z}$ are Pauli matrices on a unit-cell basis. However, in the regime where the energy spectrum is real, the Hamiltonian preserves pseudo-Hermitian symmetry [35]. The eigenvectors $|u_+\rangle$ and $|u_-\rangle$ correspond to the two bands $E_\pm(k) = \pm\epsilon(k)$, where $\epsilon(k) = \sqrt{\xi(k)^2/4 + \Delta\gamma}$ (see Fig. 2). The η-pseudo-Hermitian symmetry of the system, where $\eta = \eta_+$, has been extensively studied in previous works [21,35–38]. For energy values satisfying $\epsilon(k)^2 > 0$, the metric operator η_+ is defined by $\eta_+^{-1} = |u_+\rangle\langle u_+| + |u_-\rangle\langle u_-|$ [35]. Upon substituting these eigenvectors into the aforementioned formula and simplifying, we obtain the explicit expression for the metric operator η_+, whose inverse is given as

$$\eta_+^{-1} = \begin{bmatrix} \frac{(\xi^2(k)+2\Delta^2+2\Delta\gamma)}{\xi^2(k)+(\Delta+\gamma)^2} & \frac{\xi(k)(\gamma-\Delta)}{\xi^2(k)+(\Delta+\gamma)^2} \\ \frac{\xi(k)(\gamma-\Delta)}{\xi^2(k)+(\Delta+\gamma)^2} & \frac{\xi^2(k)+2\gamma^2+2\gamma\Delta}{\xi^2(k)+(\Delta+\gamma)^2} \end{bmatrix}, \quad (2)$$

where the pseudosymmetry matrix satisfies the relation $\eta_+ H \eta_+^{-1} = H^\dagger$, and its determinant can be expressed as $\det(\eta_+) = \frac{\xi^2(k)+(\Delta+\gamma)^2}{\xi^2(k)+4\Delta\gamma}$. Since the energy spectrum of the system is real, i.e., when the square of the energy satisfies $\xi^2(k) + 4\Delta\gamma > 0$, it follows $\det(\eta_+) > 0$. This property allows for the well-defined nature of the η_+ inner product [36]. Specifically, the η_+ inner product can be expressed as $\langle\psi|\phi\rangle_+ = \langle\psi|\eta_+|\phi\rangle$, where the set of states $\{|\phi\rangle\}$ form a Hilbert space $\mathcal{H}$ equipped with the metric η_+ [39].

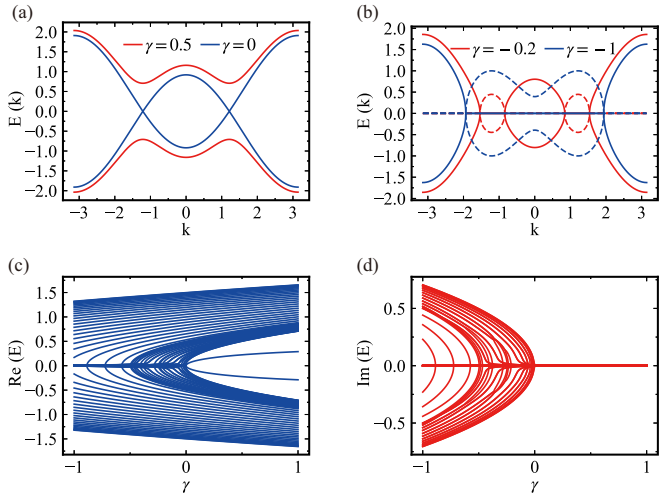

FIG. 2. (a) and (b) Energy spectrum diagram in k space with $\gamma > 0$ in (a) and $\gamma < 0$ in (b). The full line denotes the real part of the energy, and the dashed line denotes the imaginary part of the energy. The fully real energy spectra in (a) imply there is a pseudo-Hermitian symmetry when $\gamma > 0$, while that pseudo-Hermitian symmetry is broken when $\gamma < 0$ in (b). Other parameters are set as $t = 1$, $\Delta = 0.5$, $\mu = 0.7$. (c) and (d) Energy spectrum diagram in real space as a function of γ. As γ decreases, purely imaginary eigenvalues appear, indicating a transition of the system from complete pseudo-Hermitian symmetry to partial pseudo-Hermitian symmetry breaking.

The Hamiltonian in the presence of a gap exhibits a pseudo-Hermitian symmetric phase for $\Delta\gamma > 0$ due to the invariance of eigenvectors under the pseudo-Hermitian symmetry operator $\eta H^{\dagger}(k)\eta^{-1} = H(k)$ and the existence of two real energy bands in the spectrum [40]. The spectrum becomes gapless with a linear dispersion $\epsilon(k) = t \sin k_0 |k \pm k_0|$ at $\gamma\Delta = 0$, where k_0 denotes an energy gapless point $(-k_{\mathcal{EP}}, k_{\mathcal{EP}})$. An exceptional point (EP) is marked at $k = k_0$, where biorthogonal Hilbert spaces lose their completeness. In the region of real eigenvalues, the system is in a pseudo-Hermitian symmetry phase if $\cos k < (\mu - \sqrt{-4\Delta\gamma})/2$ or $\cos k > (\mu + \sqrt{-4\Delta\gamma})/2t$, while it is in a pseudo-Hermitian symmetry broken phase with conjugate pairs of imaginary eigenvalues if $(u - \sqrt{-4\Delta\gamma})/2t < \cos k < (\mu + \sqrt{-4\Delta\gamma})/2t$ for $\Delta\gamma < 0$. The regions with real spectra are separated by EPs occurring at $\epsilon(k_0) = 0$ (Fig. 2).

IV. QUANTUM TRANSPORT

On the non-Hermitian physics, the response function does not possess time-translation invariance owing to the varying density matrix $\rho(t)$ at various moments, which may exhibit a nonunitary evolution even in the absence of external perturbations. To address this issue, Sticlet *et al.* [32] and Pan *et al.* [31] have introduced a generalized response function for non-Hermitian systems, given by $\chi_{A,B}(t,t') = -i\theta(t - t')tr\{[A(\tau), B] - \langle A(t)\rangle_0[\exp(iH_0^{\dagger}\tau)\exp(-iH_0), B]\frac{\rho_0(t')}{tr\rho_0(t)}\}$. Herein, $[A, B]$ denotes the so-called generalized commutator defined as $[A, B] = AB - B^{\dagger}A$. Also, $\tau = t - t'$ represents the time interval between the initial and final states, and ρ_0 signifies the density matrix of the unperturbed system Hamiltonian H_0, which evolves with time. The formulation is obtained using the right eigenvectors of H_0.

In general, non-Hermitian dynamics may exhibit nonunitary evolution, and the density matrix of the system is not necessarily fixed at its initial value $[\rho(t) \neq \rho_0]$. Nonetheless, certain physical systems possess pseudo-Hermitian symmetry, which causes the non-Hermitian density matrix to remain unchanged at its initial value, see the Appendixes. For instance, in the pseudosymmetric phase of our system, the density matrix becomes independent of time.

In the presence of an external potential $\tilde{V}(t)$, the pseudo-Hermitian model exhibits a real eigenspectrum. The influence of an external field on a neutral atomic system can be characterized by the particle current density operator $j = -\delta H/\delta\tilde{V}$. Despite the non-Hermitian nature of the Hamiltonian, the particle current operator remains Hermitian. In this scenario, which can be regarded as a time-independent perturbation, the response function is given by

$$\begin{aligned}\chi(\tau) = &\sum_{k\in PS} i\theta(\tau)\langle[j(k,\tau), j(k,0)]\rangle_0 \\ &- \langle j(k,0)\rangle_0\langle[\exp(iH_0^{\dagger}\tau) \\ &\times \exp(-iH_0\tau), j(k,0)]\rangle_0, \end{aligned} \tag{3}$$

where the current operator j is defined as $j = -\frac{1}{2}\sum_k \partial\xi(k)/\partial k\sigma_z$. Herein, the sum over k can only be evaluated in the real spectrum, and the thermal expectation value is defined by $\langle j\rangle_0 = tr(\rho_0 j)/tr(\rho_0)$. The response function assumes a nonzero value solely in the pseudo-Hermitian symmetry phase, while remaining zero in the broken pseudo-Hermitian symmetry phase. This result follows from an exact cancellation between the generalized commutator contribution to the response $[j(k,\tau), j(k,0)]$ and the norm corrections, see the Appendixes. At zero temperature, the system exhibits a half-filled Majorana zero mode [14].

For generic real pairing order parameters, both the generalized commutator and the norm correction terms contribute to $\chi(k,\tau)$, which can be expressed as (see the Appendixes)

$$\begin{aligned}\chi(k,\tau) &= \theta(\tau)\sin^2 k \sin(2\epsilon(k)\tau)A[\epsilon(k),\xi(k)], \\ A[\epsilon(k),\xi(k)] &= \frac{128t^2\gamma^2(2\epsilon-\xi)^2}{\{4\gamma^2 + [2\epsilon(k) - \xi(k)]^2\}^2}. \end{aligned} \tag{4}$$

Notably, the Hamiltonian $H(\gamma = -\Delta) = \xi(k)/2\sigma_z + i\Delta\sigma_y$ implies that $[j(k), H] = 0$, thereby rendering the current operator time independent. As a result, the first contribution to $\chi(k,\tau)$ in Eq. (3), involving the commutator $[j(k,\tau), j(k)] = 0$, is discarded. However, the second contribution cannot be ignored. This effect is entirely non-Hermitian, a feature absent from Hermitian systems.

V. SF VISCOSITY

The time-dependent response function $\chi(\tau)$ is obtained by summation over all momentum states [Fig. 3(a)]. Our findings show that, in the pseudo-Hermitian symmetry phase, the dissipation parameter γ is positive, and $\chi(\tau)$ exhibits damped oscillation with slow decay, while in the pseudo-Hermitian

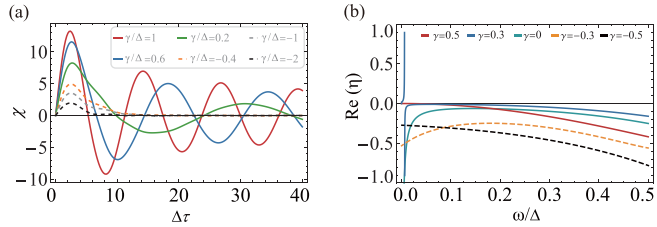

FIG. 3. (a) The spatiotemporal evolution of the response function $\chi(\tau)$ is shown, where τ represents time and γ denotes the dissipation parameter. (b) The numerical solution of the viscosity of the one-dimensional non-Hermitian zigzag bosonic chains in the frequency domain is presented for varying levels of dissipation strength. In the case of weak dissipation $0 < \gamma < \Delta$, the viscosity vanishes in the low-frequency limit. In contrast, for strong dissipation $\gamma < 0$, the viscosity in the low-frequency regime remains nonzero. The numerical parameters for (a) and (b) are set as $t = 1$, $\Delta = 0.5$, and $\mu = 0.7$.

symmetry broken phase, the γ is negative, and the response function decays exponentially. The response in frequency space $\chi(\omega)$ is obtained by Fourier transforming Eq. (3) and summing over momenta, i.e., $\chi(\omega) = \int_{k\in PS} \chi(k,\omega)$, where $\eta = 0^+$. The real part of the viscosity is given by the imaginary part of the response function, i.e., $1/\eta'(\omega) = \chi''(\omega)/\omega$, where $\chi''(\omega) = [\chi(\omega) - \chi(-\omega)]/2$ [41]. After lengthy calculation, the real-part function of the viscosity can be expressed, see the Appendixes. The viscosity curves of the EKM to an external potential are shown in Fig. 3(b).

The effects of dissipation on the viscosity response can be explained by the interplay between the SF and dissipation [42–44]. In the limit of weak dissipation ($0 < \gamma/\Delta < 1$), SFs dominate, and the system retains its energy gap. When the frequency of the external potential exceeds the energy gap, Cooper pairs are destroyed, causing SFs to be unstable under high-frequency external potential. In the case of strong dissipation ($\gamma/\Delta \ll 0$), the system is governed by the continuous quantum Zeno effect (QZE) [45–49], suppressing neighboring tunneling, leading to particle localization, and coherence of Cooper pairs is suppressed by dissipation, ultimately destroying SF. When the system resides between these two scenarios, the Cooper pairing is entirely disrupted, yet the localization induced by the QZE is insufficient to form an insulator. Under these circumstances, the system is more inclined to form a normal fluid phase.

At the critical point $\gamma = 0$, the system viscosity diverges, indicating a transition from a SF phase to a normal liquid (NL) phase. In this case, the energy spectrum becomes a linear dispersion relation $\epsilon(k) = |\xi(k)|/2 \simeq v|k - k_0|$ (see Fig. 2) near the EPs k_0, where $v = \partial\epsilon(k)/\partial k = t \sin k_0 \mathrm{sgn}(k - k_0)$ represents the group velocity. The Hamiltonian can be expressed as

$$H(k) = \begin{pmatrix} v|k - k_0| & \Delta \\ & -v|k - k_0| \end{pmatrix}. \tag{5}$$

There are only two EPs. At EPs, the Hamiltonian eigenvectors no longer constitute a complete Hilbert space, and there is only one eigenvector $|+\rangle = (1, 0)^T$. The particle current density is expressed as $j = v\langle +|\sigma_z|-\rangle = t \sin k_0 \mathrm{sgn}(k - k_0)$.

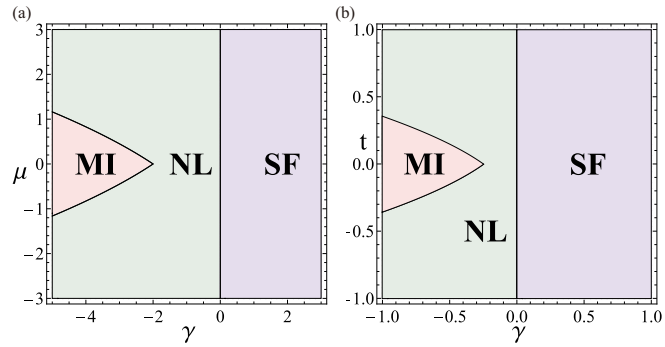

FIG. 4. (a) Phase diagram of the system parameterized by dissipation strength γ and chemical potential μ. As γ increases below zero, the system undergoes a transition from the Mott-insulator (MI) phase to the normal liquid (NL) phase. When γ exceeds zero, the system undergoes a transition from the NL phase to the superfluid (SF) phase. (b) Phase diagram of the system parameterized by dissipation strength γ and tunneling t. When $\gamma > 0$, the SF phase appears, while when $\gamma < 0$, the NL phase appears. When γ continues decreasing, the positive pseudo-Hermitian symmetry is completely broken, and the system turns into the MI phase. The numerical parameters for (a) and (b) are set as $t = 1$, $\Delta = 0.5$, and $\mu = 0.7$.

Thus, in the case of $|k| > |k_{\mathcal{EP}}|$, the particle current density is $j = t \sin k_{\mathcal{EP}}$, while in the case of $|k| < |k_{\mathcal{EP}}|$, the particle current density is $j = t \sin k_{\mathcal{EP}}$. In momentum space, currents in different regions cancel each other out.

In the non-Hermitian zigzag bosonic chains, when the dissipation strength is sufficiently large, the quasifermions are bound to the protocell due to the continuous QZE. Based on our findings, we depict phase diagrams of our system in Fig. 4. The purple region denotes the system remaining in the SF phase under weak dissipation conditions. The green region represents the SF phase being destroyed and replaced by a NL phase under strong dissipation. In the red region, the system has no real energy spectrum and no pseudo-Hermitian symmetry, and the system enters into the MI phase.

VI. EXPERIMENTAL REALIZATION

Returning to a realistic experiment with concrete parameters, we choose lattice trap potential $V_0 = 5E_R$, with $E_R = h^2/(2m\lambda_L^2) \approx 0.914$ kHz being the recoil energy as the energy unit. The intrachain hopping amplitude can be determined as $t \approx 0.0192E_R \approx 17.55$ Hz. Using the standard technique of Feshbach resonance, we can tune the bare interaction strength $g = -2.0E_R$, which leads to the Hubbard interaction strength $U \approx -8.14E_R \approx 7.44$ kHz, satisfying the limit of $U \gg t$ [50–52]. On the other hand, the interaction strength U_r for the reservoir chain can also be artificially tuned. We can choose a fixed chemical potential offset μ_0 between the chains and apply a running laser with frequency matching the energy difference $U_r - \mu_0$. This interaction-induced resonant tunneling has been implemented in experiments to investigate interacting dipoles [53,54]. At last, the imbalanced pairing parameters are induced by applying an additional laser with wavelength $\lambda = 1285$ nm to couple $^3P_0$ to $^1P_1$ resonantly, and the complex part of the pairing term can be tuned by the loss rate of excited state $|e\rangle$ [55–57]. The dynamical displacement

of atoms can be measured by single-site-resolved quantum gas microscopy [58], and the transport response can be revealed by spectroscopic probes [50,59].

VII. DISCUSSION

In summary, we have investigated the non-Hermitian SF-MI transition of zigzag bosonic chains with strong Hubbard interaction. In this paper, we have revealed that the quantum phase transition can be described by the transport behavior of 1D non-Hermitian zigzag bosonic chains under an alternating external potential. Our non-Hermitian systems are constructed from dissipative open systems, and the dissipation strength plays a crucial role in determining the impact of the non-Hermitian response function. Specifically, in the weak dissipation limit, the system retains its energy gap, with the system approaching the SF phase, whereas in the strong dissipation limit, with the QZE suppressing neighboring tunneling, the system tends toward the NL phase. As the dissipation increases further, Cooper pairs of quasifermions in the system decomposed, leading to a NL-MI phase transition. The calculation of the non-Hermitian Green's function has revealed that the viscosity of our system is contingent upon the emergence of pseudosymmetries, which is an unconventional quantum phase transition characteristic of non-Hermitian zigzag bosonic chains. Notably, these phase transitions are accompanied by the appearance and disappearance of EPs. These characteristics can be experimentally tested, and future work can further extend 1D zigzag bosonic chains to higher dimension.

ACKNOWLEDGMENTS

This work was supported by the National Key R&D Program of China under Grants No. 2021YFA1400900, No. 2021YFA0718300, and No. 2021YFA1402100, NSFC under Grants No. 12174461, No. 12234012, No. 12334012, and No. 52327808, and the Space Application System of China Manned Space Program.

APPENDIX A: NON-HERMITIAN PAIRED-BOSE-HUBBARD MODEL

Considering the two-body loss in the optical lattice, the non-Hermitian paired-Bose-Hubbard model (NHHM) Hamiltonian obtained can be written as [16,60]

$$H = -\sum_{i,j}(wb_i^\dagger b_j + \text{H.c.} + \Delta_1 b_i^\dagger b_j^\dagger + \Delta_2 b_j b_i) + \sum_i\left[\frac{U}{2}n_i(n_i-1) - \mu n_i\right], \tag{A1}$$

where U is the repulsion interaction, w is the hopping amplitude from site j to i, μ is the chemical potential, and it is worth noting that $t, U, \Delta_{1,2} \in \mathbb{R}$. In the situation of a strong coupling limit of the Hubbard model ($U \geqslant w$), this is then a model of hard-core bosons with an infinite on-site repulsion energy. The only states with a finite energy are those with $|n_0\rangle$ or $|n_0+1\rangle$ on every site of the lattice. There are only two MIs with $n = n_0$ or $n = n_0 + 1$ permitted. The hard-core paired Bose-Hubbard model can also be written as a magnet model ($s = \frac{1}{2}$) by taking transformation $|n_0+1\rangle = |\uparrow\rangle$, $|n_0\rangle = |\downarrow\rangle$, $b_i^\dagger b_j = (n_0+1)s_i^+ s_j^-$, and $n = n_0 + \frac{1}{2} + s_z$ [61]. Thus, the transverse field non-Hermitian XY model can be derived by applying degenerate perturbation theory to the second order of $\tilde{t}/U$ [6]:

$$H = \sum_{\langle i,j\rangle}\left[J_x s_i^x s_j^x + J_y s_i^y s_j^y - iJ_{xy}\left(s_i^x s_j^y + s_i^y s_j^x\right)\right] - h\sum_i s_i^z, \tag{A2}$$

where $J_x = -(n_0+1)(2w + \Delta_1 + \Delta_2)$, $J_y = -(n_0+1)(2w - \Delta_1 - \Delta_2)$ is the anisotropic spin-exchange integral, $J_{xy} = 2(\Delta_1 - \Delta_2)$ is the non-Hermitian term, and $h = \mu - Un_0$ is the Zeeman magnetic field.

The non-Hermitian XY model possesses pseudo-Hermitian symmetry $\eta = \prod_i (-1)^{n_i}$, $H^\dagger = \eta H \eta^{-1}$, which ensures the possibility of a purely real energy spectrum. The transverse field spin chain can be reformed to the fermionic Kitaev model by Jordan-Wigner transformation $s_i^+ = c_i^\dagger \exp(i\pi \sum_{j<i} c_j^\dagger c_j)$ and $s_i^- = \exp(-i\pi \sum_{j<i} c_j^\dagger c_j)c_i$. In this way, the non-Hermitian Hubbard interaction is transformed into the Kitaev model in the $t/U \to 0$ limit. By calculating the linear response of the Kitaev model, the physical properties of the NHHM near the MI phase can be obtained by

$$H = \sum_{\langle i,j\rangle}(-tc_i^\dagger c_j + \text{H.c.} + \Delta c_i^\dagger c_j^\dagger + \gamma c_i c_j) + \sum_i \mu c_i^\dagger c_i, \tag{A3}$$

where $t = (n_0+1)w$ is the hopping amplitude between the nearest-neighbor site, $\Delta = (n_0+1)\Delta_1$ and $\gamma = (n_0+1)\Delta_2$ denote the strength of the pair parameters between the nearest-neighbor sites, and μ is on-site chemical potential.

APPENDIX B: $U(1)$ TRANSFORMATION AND APPROXIMATE

We considered the case where $U \gg |\Delta|$ and made an approximation to transform into an equivalent bosonic representation.

The Hamiltonian of the bosonic zigzag chain can be written as

$$H = \sum_i \psi^\dagger H_{\text{BdG}} \psi, \tag{B1}$$

$$H_{\text{BdG}} = \sigma_x \otimes H_0, \tag{B2}$$

where $\psi^\dagger = (b_i^\dagger \quad b_i \quad b_{i+1}^\dagger \quad b_{i+1})$, $H_0 = \begin{bmatrix} w & \Delta \\ \Delta & w \end{bmatrix}$.

We decompose H_0 into two parts, where $H_0 = H_1 + H_2$ and $H_1 = \begin{pmatrix} w & \text{Re}\Delta \\ \text{Re}\Delta & w \end{pmatrix}$, $H_2 = \begin{pmatrix} 0 & i\text{Im}\Delta \\ i\text{Im}\Delta & 0 \end{pmatrix}$. According to the method of realizing complex matrices found in the article by Ikramov [62], we can further perform a unitary transformation:

$$W^\dagger H_2 W = \begin{bmatrix} w & \text{Im}\Delta \\ -\text{Im}\Delta & w \end{bmatrix}, \tag{B3}$$

where $W = \exp[i\pi/2(\frac{1}{2} - \sigma_n)]$ and $\hat{n} = (\sqrt{2}/2, \sqrt{2}/2)$. At the same time, we can find that

$$W^\dagger H_2 W = \exp\left[i\frac{\pi}{2}\left(\frac{1}{2} - \sigma_n\right)\right] H_2 \exp\left[-i\frac{\pi}{2}\left(\frac{1}{2} - \sigma_n\right)\right] = U^\dagger H_2 U, \tag{B4}$$

where $U = \exp(-i\frac{\pi}{2}\sigma_n)$. Using the Baker-Campbell-Hausdorff formula:

$$e^A B e^{-A} = B + [A, B] + \frac{1}{2!}[A, [A, B]] + \cdots, \tag{B5}$$

we can calculate to obtain

$$W^\dagger H_2 W = H_2 - i\mathrm{Im}\Delta\frac{\sqrt{2}\pi}{2}\sigma_z + i\mathrm{Im}\Delta\frac{\pi^2}{4}. \tag{B6}$$

In the problem we are interested in, we are studying the dynamic response in the large U limit. This means that $\mathrm{Im}\Delta/U \to 0$, so in this specific problem, we used the approximation $H_2 \sim W^\dagger H_2 W$.

Under this approximation, the original Hamiltonian can be transformed into an equivalent asymmetric pairing Hubbard model:

$$H = -\sum_{i,j}(wb_i^\dagger b_j + \mathrm{H.c.} + \Delta_1 b_i^\dagger b_j^\dagger + \Delta_2 b_j b_i) + \sum_i\left[\frac{U}{2}n_i(n_i - 1) - \mu n_i\right], \tag{B7}$$

where $\Delta_1 = \mathrm{Re}\Delta + \mathrm{Im}\Delta$, $\Delta_2 = \mathrm{Re}\Delta - \mathrm{Im}\Delta$, and $n_i = b_i^\dagger b_i$.

APPENDIX C: PSEUDOSYMMETRY SYSTEM

Since H is nonhermitic, it has a biorthogonal basis $|u\rangle$, $|v\rangle$, which satisfies

$$H|u_i\rangle = E_i|u_i\rangle, \quad \langle u_i|H^\dagger = E_i^*\langle u_i|,$$
$$H|v_i\rangle = R_i|v_i\rangle, \quad \langle v_i|H^\dagger = R_i^*\langle v_i|, \tag{C1}$$

$$\langle v_i|u_j\rangle = \delta_{ij}, \tag{C2}$$

The metric operators $\eta = \sum_i |v_i\rangle\langle v_i|$ and $\eta^{-1} = \sum_i |u_i\rangle\langle u_i|$ related $|u_i\rangle$ and $|v_i\rangle$:

$$|v_i\rangle = \eta|u_i\rangle, \quad |u_i\rangle = \eta^{-1}|v_i\rangle. \tag{C3}$$

Using this relation, we can define the η inner product between the Hilbert space $\mathcal{H}$ corresponding to the eigenvector $|u_i\rangle$ and the Hilbert space $\mathcal{H}^*$ corresponding to the eigenvector $\langle v_i|$:

$$\langle v_i|u_j\rangle = \langle u_i|\eta|u_j\rangle = \langle u_i|u_j\rangle_\eta = \delta_{ij}, \tag{C4}$$

where $\langle\cdot|\cdot\rangle_\eta$ is called the η product.

It has been proven in Refs. [40,63,64] that the necessary and sufficient conditions for a non-Hermitian but diagonalizable Hamiltonian to have real eigenvalues is the existence of a linear positive-definite operator $\eta(\det\eta > 0)$ such that $\eta H\eta^{-1} = H^\dagger$ is fulfilled.

The quasifermion EKM in lattice space is written as

$$H = \sum_{\langle i,j\rangle} -tc_i^\dagger c_j + \mathrm{H.c.} + \Delta c_i^\dagger c_j^\dagger + \gamma c_i c_j + \sum_i \mu c_i^\dagger c_i. \tag{C5}$$

Taking Fourier transformation $c_n = 1/\sqrt{N}\sum_k \exp(ik\cdot R_n)c_k$, the Hamiltonian in k space is described by

$$H = \sum_k (c_k^\dagger c_{-k})\begin{bmatrix}\frac{\xi(k)}{2} & \Delta \\ \gamma & -\frac{\xi(k)}{2}\end{bmatrix}\begin{pmatrix}c_k \\ c_{-k}^\dagger\end{pmatrix}, \tag{C6}$$

where $\xi(k) = \mu - 2t\cos k$ and $H(k) = \xi(k)\sigma_z/2 + (\Delta + \gamma)\sigma_x/2 + i(\Delta - \gamma)\sigma_y/2$. The lattice constant we defined is the unit, and the lattice constant a and Planck constant $\hbar$ we set as the unit ($a = \hbar = 1$). The eigenvalue and the eigenvector of H can be solved, respectively, to obtain

$$E_\pm(k) = \pm\frac{\sqrt{\xi^2(k) + 4\Delta\gamma}}{2}, \quad |u_\pm\rangle = \left\{\frac{-\xi(k)\pm\sqrt{\xi^2(k)+4\Delta\gamma}}{\sqrt{4\gamma^2+[-\xi(k)\pm\sqrt{\xi^2(k)+4\Delta\gamma}]^2}} \quad \frac{2\gamma}{\sqrt{4\gamma^2+[-\xi(k)\pm\sqrt{\xi^2(k)+4\Delta\gamma}]^2}}\right\}. \tag{C7}$$

We calculate the value of η:

$$\eta = |u_+\rangle\langle u_+| + |u_-\rangle\langle u_-| = \left\{\frac{[\xi^2(k)+2\Delta^2+2\Delta\gamma]}{\xi^2(k)+(\Delta+\gamma)^2} \quad \frac{\xi(k)(\gamma-\Delta)}{\xi^2(k)+(\Delta+\gamma)^2} \quad \frac{\xi(k)(\gamma-\Delta)}{\xi^2(k)+(\Delta+\gamma)^2} \quad \frac{\xi^2(k)+2\gamma^2+2\gamma\Delta}{\xi^2(k)+(\Delta+\gamma)^2}\right\}, \tag{C8}$$

where $\eta H\eta^{-1} = H^\dagger$ is satisfied. The determinant of η is

$$\det(\eta) = \frac{\xi^2(k) + 4\Delta\gamma}{\xi^2(k) + (\Delta+\gamma)^2}. \tag{C9}$$

Systems with η pseudo-Hermitian symmetries have real energy spectra for $\det(\eta) > 0$.

APPENDIX D: THE CALCULATION OF THE RESPONSE FUNCTION

The non-Hermitian is written as

$$H = H_0 + V(t), \quad V(t) = Bf(t), \tag{D1}$$

where $V(t)$ is perturbation, and H_0 is the nonperturbation Hamiltonian. There is no restriction here on the hermiticity of perturbation B.

The generalized response function in a non-Hermitian system is described by [31,32]

$$\chi_{A,B}(t,t') = -i\theta(t-t')tr\left\{[A(\tau), B] - \langle A(t)\rangle_0 \times [\exp(iH_0^\dagger\tau)\exp(-iH_0), B]\frac{\rho_0(t')}{tr\rho_0(t)}\right\}, \tag{D2}$$

where the commutator $[A, B]$, which is called the generalized commutator, is defined by $[A, B] = AB - B^\dagger A$, and $\tau = t - t'$ represents a time interval between the initial and final states and the density matrix of the nonperturbation system Hamiltonian H_0 denoted by ρ_0 which is time dependent.

In the non-Hermitian model, the response function has no time-transition invariant due to the appearance of the system density matrix $\rho(t)$ at various times, which may have a nonunitary evolution in the absence of perturbation.

At the initial time, the nonnormalized density matrix can be written in terms of the eigenstates ($|\psi_k\rangle$, $\langle\psi_k|$) of any Hermitian operator, defined in the Hilbert space of the subsystem, and of their statistical weights w_k:

$$\rho_0 = \sum_i w_i |\psi_i\rangle\langle\psi_i|, \tag{D3}$$

where $\sum_k w_k = 1$.

However, if we consider the system is in the pseudosymmetry phase, there is a real energy spectrum in the system. In this case, the density matrix ρ evolves over time in the form:

$$\rho_0(\tau) = \sum_k w_k \exp(-iH_0\tau)|\psi_i\rangle\langle\psi_i|\exp(iH_0^\dagger\tau) = \rho_0. \tag{D4}$$

Thus, we get the conclusion that the density matrix is time independent in the pseudosymmetry phase.

With a real eigenspectrum in a pseudo-Hermitian system, under a time-dependent perturbation $V(t) = Bf(t)$, the correlation function can be reduced as

$$\begin{aligned}\chi_{A,B}(\tau) = &-i\theta(\tau)\{\langle[A(\tau), B(0)]\rangle_0 - \langle A(0)\rangle_0 \\ &\times \langle[\exp(iH_0^\dagger\tau)\exp(-iH_0\tau), B(0)]\rangle_0\},\end{aligned} \tag{D5}$$

where $\chi_{A,B}(\tau)$ is the pseudo-Hermitian response of A, B. Note that the above formula is in the interaction picture. The thermal expectation is defined by $\langle A\rangle_0 = tr(\rho_0 A)/tr(\rho_0)$. The response function has a value only in the unbroken phase of pseudo-Hermitian symmetry and is zero in the pseudo-Hermitian symmetry-broken phase. This is due to exact cancellation between the generalized commutator contribution to the response $[j(k,\tau), j(k,0)]$ and the norm corrections.

For the EKM now, let $j = -\frac{1}{2}\sum_k \partial\xi(k)/\partial k\sigma_z$, and the response function is written

$$\begin{aligned}\chi(\tau) = &\sum_{k\in PS} i\theta(\tau)\langle[j(k,\tau), j(k,0)]\rangle_0 \\ &- \langle j(k,0)\rangle_0\langle[\exp(iH_0^\dagger\tau)\exp(-iH_0\tau), j(k,0)]\rangle_0,\end{aligned} \tag{D6}$$

where the sum over k can only be calculated in the real spectrum. At zero temperature, the system is half-full.

For generic real pairing order parameters Δ, γ, both the generalized commutator and the norm correction terms contribute. We choose the ground state $|u_-\rangle$ of Hamiltonian $H(k)$ in Eq. (C7):

$$\langle[j(k,\tau), j(k,0)]\rangle_0 = \langle j(k,\tau)j(k,0) - j^\dagger(k,0)j(k,\tau)\rangle_0 = -\frac{8it^2\gamma(\Delta+\gamma)[2\epsilon(k)-\xi(k)]\sin[2\epsilon(k)t]\sin^2 k}{\epsilon(k)\{2\gamma^2+2\gamma\Delta+\xi(k)[\xi(k)-2\epsilon(k)]\}}, \tag{D7}$$

$$\langle j(k,0)\rangle_0 = -\frac{2t\{2\gamma^2-2\gamma\Delta+\xi(k)[2\epsilon(k)-\xi(k)]\}\sin k}{2\gamma^2+2\gamma\Delta+\xi(k)[\xi(k)-2\epsilon(k)]}, \tag{D8}$$

$$\langle[\exp(iH_0^\dagger\tau)\exp(-iH_0\tau), j(k,0)]\rangle_0 = \frac{4it\gamma(\gamma-\Delta)(2\epsilon-\xi)\sin[2\epsilon(k)\tau]\sin k}{\epsilon(k)\{2\gamma^2+2\gamma\Delta+\xi(k)[\xi(k)-2\epsilon(k)]\}}. \tag{D9}$$

Substituted into Eq. (D6), the result can be derived:

$$\chi(k,\tau) = \theta(\tau)\sin^2 k\sin 2\epsilon(k)\tau A[\epsilon(k),\xi(k)], \tag{D10}$$

$$A[\epsilon(k),\xi(k)] = \frac{128t^2\gamma^2[2\epsilon(k)-\xi(k)]^2}{\{\epsilon(k)[2\epsilon(k)-\xi(k)]-\gamma(\Delta-\gamma)\}^2}, \tag{D11}$$

where $\xi(k) = \mu - 2t\cos k$ is the kinetic energy term, and $\epsilon(k) = \sqrt{\xi^2(k)/4+\Delta\gamma}$ is the absolute value of the energy eigenvalue.

APPENDIX E: VISCOSITY

The time-dependent $\chi(\tau)$ is obtained by summation over all momentum states. The response function $\chi(\tau)$ of the system exhibits a damped oscillating behavior with a slow decay in the pseudosymmetry phase of $\gamma > 0$. The $\chi(\tau)$ response function decays exponentially and vanishes rapidly in the pseudosymmetry phase of $\gamma < 0$. The response in frequency space $\chi(\omega)$ follows by Fourier transforming. Putting $\theta(\tau) = \lim_{\eta->0^+}\int \frac{\exp(i\omega\tau)}{\omega-i\eta}\frac{d\omega}{2\pi i}$ into Eq. (D6), we can obtain

$$\begin{aligned}\chi(k,\omega) = \int d\tau\,\chi(k,\tau)\exp(i\omega\tau) = &\frac{1}{2}\sin^2 kA[\epsilon(k),\xi(k)] \\ &\times\left[\frac{1}{\omega+2\epsilon(k)+i\eta} - \frac{1}{\omega-2\epsilon(k)+i\eta}\right].\end{aligned} \tag{E1}$$

Summing over all the real energy spectrum momenta,

$$\chi(\omega) = \int_{k\in PS}\chi(k,\omega). \tag{E2}$$

The real part of the viscosity is given by the imaginary part of the response function $\sigma'(\omega) = \chi''(\omega)/\omega$, where $\chi''(\omega) = [\chi(\omega)-\chi(-\omega)]/2i$ [41],

$$\begin{aligned}\chi''(\omega) &= -\frac{\pi}{2}\int_{k\in PS} dk\sin^2 kA(k)[\delta(\omega-2\epsilon)-\delta(\omega+2\epsilon)] \\ &= -\frac{\pi}{2}\int_{k\in PS} dk\delta[\omega-2\epsilon(k)]\sin^2 kA(k) \\ &= -\frac{\pi}{2}\int_{k\in PS} dk\delta(k-k_i)\frac{\epsilon(k_i)}{t\xi(k_i)\sin k_i}\sin^2 kA(k), \\ &\quad\times[\omega>0, \epsilon(k)>0, k_i = k_1, k_2],\end{aligned} \tag{E3}$$

where k_i satisfies $\omega = 2\epsilon(k_i)$ and the above first line is used $1/(x+i\eta) = P(1/x) - i\pi\delta(x)$:

$$\begin{aligned}k_1 &= \arccos\frac{\mu+\sqrt{\omega^2-4\Delta\gamma}}{2t}, \\ k_2 &= \arccos\frac{\mu-\sqrt{\omega^2-4\Delta\gamma}}{2t},\end{aligned} \tag{E4}$$

(1) $\frac{\mu+\sqrt{-4\Delta\gamma}}{2t} < 1$ and $\frac{\mu-\sqrt{-4\Delta\gamma}}{2t} > -1$:

$$\chi''(\omega) = -\frac{\pi}{2}\left(\frac{\epsilon(k_1)}{\xi(k_1)}\sin k_1 \frac{128t\gamma^2[2\epsilon(k_1)-\xi(k_1)]^2}{\{\gamma^2+[2\epsilon(k_1)-\xi(k_1)]^2\}^2} + \frac{\epsilon(k_2)}{\xi(k_2)}\sin k_2 \frac{128t\gamma^2[2\epsilon(k_2)-\xi(k_2)]^2}{\{\gamma^2+[2\epsilon(k_2)-\xi(k_2)]^2\}^2}\right). \tag{E5}$$

(2) $\frac{\mu+\sqrt{-4\Delta\gamma}}{2t} > 1$ and $\frac{\mu-\sqrt{-4\Delta\gamma}}{2t} > -1$:

$$\chi''(\omega) = -\frac{\pi}{2}\left(\frac{\epsilon(k_2)}{\xi(k_2)}\sin k_2 \frac{128t\gamma^2[2\epsilon(k_2)-\xi(k_2)]^2}{\{\gamma^2+[2\epsilon(k_2)-\xi(k_2)]^2\}^2}\right). \tag{E6}$$

(3) $\frac{\mu+\sqrt{-4\Delta\gamma}}{2t} > 1$ and $\frac{\mu-\sqrt{-4\Delta\gamma}}{2t} < -1$:

$$\chi''(\omega) = 0. \tag{E7}$$

APPENDIX F: PHASE DIAGRAM

The pseudosymmetry operator can be written as

$$\eta = \begin{Bmatrix} \frac{[\xi^2(k)+2\Delta^2+2\Delta\gamma]}{\xi^2(k)+(\Delta+\gamma)^2} & \frac{\xi(k)(\gamma-\Delta)}{\xi^2(k)+(\Delta+\gamma)^2} \\ \frac{\xi(k)(\gamma-\Delta)}{\xi^2(k)+(\Delta+\gamma)^2} & \frac{\xi^2(k)+2\gamma^2+2\gamma\Delta}{\xi^2(k)+(\Delta+\gamma)^2} \end{Bmatrix}, \tag{F1}$$

$$\det(\eta) = \frac{\xi^2(k)+4\Delta\gamma}{\xi^2(k)+(\Delta+\gamma)^2}. \tag{F2}$$

If the system is in pseudo-Hermitian symmetric phase, the system has a real energy spectrum. In the real spectrum, the pseudo-Hermitian operator is positive definite, that is, $\det(\eta) > 0$:

$$(\mu - 2t\cos k)^2 > -4\Delta\gamma, \quad \cos k < \frac{\mu - 2\sqrt{-\Delta\gamma}}{2t}, \quad \cos k > \frac{\mu + 2\sqrt{-\Delta\gamma}}{2t}. \tag{F3}$$

For the case where pseudohermitic symmetry is completely destroyed, the system is in the insulator phase. There are conditions:

$$\frac{\mu - 2\sqrt{-\Delta\gamma}}{2t} < -1, \quad \frac{\mu + 2\sqrt{-\Delta\gamma}}{2t} > -1. \tag{F4}$$

For the case where $\gamma > 0$, the low-frequency limit viscosity approaches infinity, which means that the system is in the superconducting phase (Fig. 5).

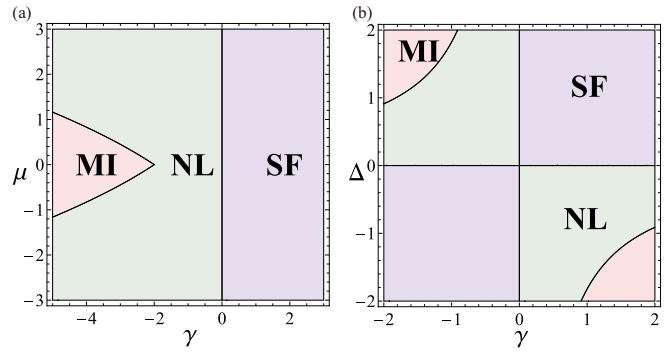

FIG. 5. The phase diagram of our system. As γ gradually increases, the system changes from an insulator phase to a normal liquid (NL) phase and eventually to a superfluid (SF) phase. The parameters are set to $t = 1$, $\Delta = 0.5$.

[1] V. E. Colussi, F. Caleffi, C. Menotti, and A. Recati, Phys. Rev. Lett. **130**, 173002 (2023).
[2] J. Fraxanet, D. González-Cuadra, T. Pfau, M. Lewenstein, T. Langen, and L. Barbiero, Phys. Rev. Lett. **128**, 043402 (2022).
[3] S. Basak and H. Pu, Phys. Rev. A **104**, 053326 (2021).
[4] Z. Meng, L. Wang, W. Han, F. Liu, K. Wen, C. Gao, P. Wang, C. Chin, and J. Zhang, Nature (London) **615**, 231 (2023).
[5] T. D. Kühner, S. R. White, and H. Monien, Phys. Rev. B **61**, 12474 (2000).
[6] S. Vishveshwara and D. M. Weld, Phys. Rev. A **103**, L051301 (2021).
[7] W. Han, G. Juzeliūnas, W. Zhang, and W.-M. Liu, Phys. Rev. A **91**, 013607 (2015).
[8] G. Liu, S.-L. Zhu, S. Jiang, F. Sun, and W.-M. Liu, Phys. Rev. A **82**, 053605 (2010).
[9] H. Shiba, Phys. Rev. B **6**, 930 (1972).
[10] Y.-H. Chen, H.-S. Tao, D.-X. Yao, and W.-M. Liu, Phys. Rev. Lett. **108**, 246402 (2012).
[11] Y.-C. Zhang, X.-F. Zhou, X. Zhou, G.-C. Guo, H. Pu, and Z.-W. Zhou, Phys. Rev. A **91**, 043633 (2015).
[12] M. Yan, Y. Qian, H.-Y. Hui, M. Gong, C. Zhang, and V. W. Scarola, Phys. Rev. A **96**, 053619 (2017).
[13] X.-M. Zhao, C.-X. Guo, M.-L. Yang, H. Wang, W.-M. Liu, and S.-P. Kou, Phys. Rev. B **104**, 214502 (2021).
[14] X.-M. Zhao, C.-X. Guo, S.-P. Kou, L. Zhuang, and W.-M. Liu, Phys. Rev. B **104**, 205131 (2021).
[15] M. R. Peterson, C. Zhang, S. Tewari, and S. Das Sarma, Phys. Rev. Lett. **101**, 150406 (2008).
[16] K. Yamamoto, M. Nakagawa, K. Adachi, K. Takasan, M. Ueda, and N. Kawakami, Phys. Rev. Lett. **123**, 123601 (2019).
[17] A. Lazarides, S. Roy, F. Piazza, and R. Moessner, Phys. Rev. Res. **2**, 022002(R) (2020).
[18] X.-W. Luo and C. Zhang, Phys. Rev. Lett. **123**, 073601 (2019).
[19] Z. Ren, D. Liu, E. Zhao, C. He, K. K. Pak, J. Li, and G.-B. Jo, Nat. Phys. **18**, 385 (2022).
[20] D. C. Brody, J. Phys. A: Math. Theor. **47**, 035305 (2014).
[21] T. Ohlsson and S. Zhou, Phys. Rev. A **103**, 022218 (2021).
[22] F. Roccati, G. M. Palma, F. Bagarello, and F. Ciccarello, Open Syst. Inf. Dyn. **29**, 2250004 (2022).
[23] X. Z. Zhang and Z. Song, Phys. Rev. B **104**, 094301 (2021).

[24] Q. Liang, D. Xie, Z. Dong, H. Li, H. Li, B. Gadway, W. Yi, and B. Yan, Phys. Rev. Lett. **129**, 070401 (2022).
[25] W. Lai, Y.-Q. Ma, L. Zhuang, and W.-M. Liu, Phys. Rev. Lett. **122**, 223202 (2019).
[26] G.-B. Zhu, Q. Sun, Y.-Y. Zhang, K. S. Chan, W.-M. Liu, and A.-C. Ji, Phys. Rev. A **88**, 023608 (2013).
[27] A. Sergi and K. G. Zloshchastiev, Int. J. Mod. Phys. B **27**, 1350163 (2013).
[28] A. Sergi and K. G. Zloshchastiev, Phys. Rev. A **91**, 062108 (2015).
[29] C.-Y. Ju, A. Miranowicz, G.-Y. Chen, and F. Nori, Phys. Rev. A **100**, 062118 (2019).
[30] W. Wu, Y.-H. Chen, H.-S. Tao, N.-H. Tong, and W.-M. Liu, Phys. Rev. B **82**, 245102 (2010).
[31] L. Pan, X. Chen, Y. Chen, and H. Zhai, Nat. Phys. **16**, 767 (2020).
[32] D. Sticlet, B. Dóra, and C. P. Moca, Phys. Rev. Lett. **128**, 016802 (2022).
[33] W. Yi, A. Daley, G. Pupillo, and P. Zoller, New J. Phys. **10**, 073015 (2008).
[34] F. Gerbier and J. Dalibard, New J. Phys. **12**, 033007 (2010).
[35] O. Cherbal, D. Trifonov, and M. Zenad, Int. J. Theor. Phys. **55**, 5318 (2016).
[36] T. Ohlsson and S. Zhou, J. Math. Phys. **61**, 052104 (2020).
[37] M. Lein and K. Sato, Phys. Rev. B **100**, 075414 (2019).
[38] J. Wang, W. Zheng, and Y. Deng, Phys. Rev. A **102**, 043323 (2020).
[39] B. Choutri, O. Cherbal, F. Ighezou, and M. Drir, Int. J. Theor. Phys. **56**, 1595 (2017).
[40] A. Mostafazadeh, J. Math. Phys. **43**, 205 (2002).
[41] K. T. Geier and P. Hauke, PRX Quantum **3**, 030308 (2022).
[42] A. J. Leggett, J. Phys. Colloques **41**, C7-19 (1980).
[43] A. J. Leggett, *Modern Trends in the Theory of Condensed Matter* (Springer, Berlin, Heidelberg, 1980), pp. 13–27.
[44] P. Noziöres and S. Schmitt-Rink, J. Low Temp. Phys. **59**, 195 (1985).
[45] N. Syassen, D. M. Bauer, M. Lettner, T. Volz, D. Dietze, J. J. Garcia-Ripoll, J. I. Cirac, G. Rempe, and S. Durr, Science **320**, 1329 (2008).
[46] M. J. Mark, E. Haller, K. Lauber, J. G. Danzl, A. Janisch, H. P. Büchler, A. J. Daley, and H.-C. Nägerl, Phys. Rev. Lett. **108**, 215302 (2012).
[47] G. Barontini, R. Labouvie, F. Stubenrauch, A. Vogler, V. Guarrera, and H. Ott, Phys. Rev. Lett. **110**, 035302 (2013).
[48] B. Zhu, B. Gadway, M. Foss-Feig, J. Schachenmayer, M. Wall, K. R. Hazzard, B. Yan, S. A. Moses, J. P. Covey, D. S. Jin *et al.*, Phys. Rev. Lett. **112**, 070404 (2014).
[49] T. Tomita, S. Nakajima, I. Danshita, Y. Takasu, and Y. Takahashi, Sci. Adv. **3**, e1701513 (2017).
[50] M. Greiner, O. Mandel, T. Esslinger, T. W. Hänsch, and I. Bloch, Nature (London) **415**, 39 (2002).
[51] M. Anderlini, P. J. Lee, B. L. Brown, J. Sebby-Strabley, W. D. Phillips, and J. V. Porto, Nature (London) **448**, 452 (2007).
[52] S. Sugawa, K. Inaba, S. Taie, R. Yamazaki, M. Yamashita, and Y. Takahashi, Nat. Phys. **7**, 642 (2011).
[53] J. Simon, W. S. Bakr, R. Ma, M. E. Tai, P. M. Preiss, and M. Greiner, Nature (London) **472**, 307 (2011).
[54] U. Bissbort, F. Deuretzbacher, and W. Hofstetter, Phys. Rev. A **86**, 023617 (2012).
[55] Y. Xu, S.-T. Wang, and L.-M. Duan, Phys. Rev. Lett. **118**, 045701 (2017).
[56] Z. Gong, Y. Ashida, K. Kawabata, K. Takasan, S. Higashikawa, and M. Ueda, Phys. Rev. X **8**, 031079 (2018).
[57] S. Lapp, J. Ang'ong'a, F. A. An, and B. Gadway, New J. Phys. **21**, 045006 (2019).
[58] M. Miranda, R. Inoue, Y. Okuyama, A. Nakamoto, and M. Kozuma, Phys. Rev. A **91**, 063414 (2015).
[59] G. K. Campbell, J. Mun, M. Boyd, P. Medley, A. E. Leanhardt, L. G. Marcassa, D. E. Pritchard, and W. Ketterle, Science **313**, 649 (2006).
[60] A. J. Daley, Adv. Phys. **63**, 77 (2014).
[61] S. Sachdev, Phys. World **12**, 33 (1999).
[62] Kh. D. Ikramov, Dokl. Akad. Nauk SSSR **430**, 15 (2010) [Dokl. Math. **81**, 8 (2010)].
[63] A. Mostafazadeh, J. Math. Phys. **43**, 2814 (2002).
[64] A. Mostafazadeh, J. Math. Phys. **43**, 3944 (2002).